PHYSICAL REVIEW A **78**, 021201(R) (2008)

From fission to explosion: Momentum-resolved survey over the Rayleigh instability barrier

M. Hoener,[1] C. Bostedt,[1,*] S. Schorb,[1] H. Thomas,[1] L. Foucar,[2] O. Jagutzki,[2] H. Schmidt-Böcking,[2] R. Dörner,[2] and T. Möller[1]

[1]*Institut für Optik und Atomare Physik, Technische Universität Berlin, Eugene-Wigner-Building EW 3-1, Hardenbergstrasse 36, 10623 Berlin, Germany*

[2]*Institut für Kernphysik, Universität Frankfurt, Frankfurt, Germany*

(Received 10 June 2008; revised manuscript received 9 July 2008; published 18 August 2008)

The spatial fragmentation patterns of clusters have been investigated around the Rayleigh instability barrier with a momentum-resolving reaction microscope akin to cold target recoil ion momentum spectroscopy (COLTRIMS). Liquidlike Ne and solid Xe clusters are studied in order to alter the short-range interaction. In the fission regime the neon clusters show spatially anisotropic fragmentation from an expanded geometry as predicted by the liquid drop model, whereas the xenon data suggest a charge separation from neighboring atom positions. For cluster explosion, both systems exhibit an isotropic fragment distribution in agreement with theoretical predictions. The results show how the atom mobility influences the fragmentation dynamics.

DOI: 10.1103/PhysRevA.78.021201 PACS number(s): 36.40.Qv, 36.40.Wa, 82.33.Fg

The fragmentation of multiply charged finite systems driven by long-range Coulomb (or pseudo-Coulomb) forces encompasses nuclei, clusters, proteins, nanostructures, droplets, and optical molasses [1]. To describe such multiply charged systems, the liquid drop model (LDM), originally formulated by Lord Rayleigh in 1882 [2], has developed into a tremendously successful tool. In brief, the LDM describes stability criteria for homogeneously charged droplets by comparing their repulsive (Coulomb) and cohesive (surface) energies. The relative contributions of the energies are characterized through the fissility parameter $X=E_{\mathrm{Coulomb}}/(2\cdot E_{\mathrm{surface}})$. The Rayleigh instability barrier of $X=1$ separates the fission regime $X<1$, where thermally activated fission over the barrier prevails, from the explosion regime $X>1$, where barrierless fragmentation channels open up [1].

In a recent series of theoretical studies Last, Levy, and Jortner have investigated the fragmentation processes of multiply charged Morse clusters around the Rayleigh instability barrier X [1,3,4]. The energetics of the clusters are described within the LDM and the fragmentation processes are analyzed with molecular dynamics simulations. Last *et al.* found that in particular the spatial distribution of fragments depends sensitively on the fissility parameter. For $X<1$ spatially anisotropic fission into few large fragments with low kinetic energies is found, while for $X>1$ a spatially isotropic Coulomb explosion into a large number of small ionic fragments with high kinetic energy is predicted.

Despite the universality of Rayleigh's concept [1], only little is known about the fragmentation geometry of multiply charged systems around the instability barrier $X=1$. Well-investigated systems such as nuclei ($X<0.7$) [1] and protein mass spectrometry ($X<0.1$) [4] manifest fission. Only recently have fission dynamics of microdroplets been investigated up to the Rayleigh limit of $X=1$ [5,6]. For clusters and other atomic systems, typically the extreme limits of fission [7,8] or explosion [9] are probed.

We have performed spatially resolved experimental investigation on the fragmentation geometry around the Rayleigh instability barrier $X=1$. For the study, two different systems are used, namely, liquidlike Ne and solid Xe clusters, in order to alter the influence of the short-range, nearest-neighbor interaction. Rare gas clusters are chosen because they allow versatile adjustment of the fissility parameter around the Rayleigh barrier by change in the cluster size and the number of deposited charges on the system. We find that for $X>1$ both systems exhibit an isotropic fragment distribution, characteristic for Coulomb explosion. In the fission regime $X<1$, however, differences in the fragmentation geometry and energetics between the liquid and solid systems become apparent.

In more detail, the fissility parameter can be calculated within the classical LDM according to [1,5]

$$X_{\mathrm{LDM}}=Z^2/(64\pi^2\epsilon_0\sigma a_0^3)=\left(\frac{Z^2}{N}\right)\Big/\left(\frac{Z^2}{N}\right)_{\mathrm{critical}} \quad (1)$$

where $\sigma=0.0051(0.019)\ \mathrm{J/m^2}$ is the surface tension of neon [10] (xenon [11]), a_0 is the cluster radius, Z is the charge on the cluster, and N the number of atoms in the cluster. In the following discussion the charge Z on the cluster will be for practical reasons measured in the number of electron charges q. Often the appearance size for a given charge state is determined in the literature; this is defined as the minimum size at which energy barriers exist for the fragmentation channels, i.e., by definition $X=1$ [1]. Based on the appearance sizes the dimensionless factor $1/(Z^2/N)_{\mathrm{critical}}$ can be deduced. The numbers resulting from measurements are 72 for Ne [7] and 12.75 for Xe [12]. Experimentally the fissility parameter can be tuned by changing the cluster size and the deposition of a defined amount of charges on it. The clusters are prepared by an adiabatic expansion of either Ne or Xe gas through a 100 μm conical nozzle with half opening angle of 15°. The cluster sizes are altered by changing the stagnation pressure and nozzle temperature and their average size $\langle N\rangle$ is determined according to the Hagena scaling laws [13,14]. The amount of charge on the cluster is tuned through photoexci-

*Corresponding author. bostedt@physik.tu-berlin.de

TABLE I. Summary of the experimental parameters and resulting fissility parameters according to the classical liquid drop model, X_{classic}, and experimental observations of appearance sizes, X_{app}.

Element	Size $\langle N \rangle$	$h\nu$ (eV)	q (unit of e)	X_{classic}	X_{app}
Ne	370	80	2	1.8	0.8
	60	890	2	11.1	4.8
			3	25.1	10.8
Xe	70	80	2	1.0	0.7
			3	2.1	1.6
	70	1160	6	8.6	6.6
			7	11.7	8.9

tation of different core electrons. The core holes decay via radiative or Auger processes and the created charges are subsequently redistributed to neighboring atoms in the cluster [15,16]. In the following discussion only the dominant highest-charge state is considered through a coincidence trigger and postanalysis. The distribution of charge states has been determined by also measuring atomic Ne and Xe at the corresponding photon energies. Further, it has been considered that the charge state of the cluster may be increased by 1 through inter-Coulombic decay (ICD) [17] compared to the atom if the Auger decay results in a hole below the valence shell. First, the clusters are excited with a photon energy of $h\nu$=80 eV leading to charge states of 2^+ for Ne through double ionization or ICD [17]. For Xe the Auger decay leads predominantly to a final state of 2^+ but in about 30% of the cases Auger and ICD processes can lead to a final charge state of 3^+ [17,18]. At photon energies above the Ne 1s level at $h\nu$=890 eV, in about 70% of the cases Auger decay leads to two charges and in 30% of the cases Auger decay with subsequent ICD can lead to three charges deposited on the cluster [17,19]. For Xe at $h\nu$=1160 eV for about 80% of the excitations there are six charges generated on the cluster and for about 10% there are seven charges. The experimental parameters and the resulting fissility parameters based on the classical LDM X_{classic} are summarized in Table I. Additionally, the fissility parameters X_{app} deduced from experimental observations of appearance sizes [7,12] as described above have been added. In the following discussion X_{app} based on measurements is used as the fissility parameter X because it most closely describes the investigated systems. For Ne fission, a cluster with $\langle N \rangle$=370 (explosion, $\langle N \rangle$=60) and a final charge state of 2 is considered. In this size regime Ne clusters are still liquidlike [20]. The Xe parameters are chosen to yield as similar X_{app} as possible compared to the Ne system within the accessible parameter space. Therefore, Xe clusters with $\langle N \rangle$=70 and final charge states of 2 (fission) and 6 (explosion) are taken.

The experiments were performed at the undulator beamline BW3 of HASYLAB at DESY in Hamburg (Germany) [21]. As detector a multihit-capable reaction microscope akin to a cold target recoil ion momentum spectroscopy (COLTRIMS) spectrometer is used [22,23] which has been optimized for the special requirements of cluster experiments. In COLTRIMS experiments the cluster-light interaction zone is

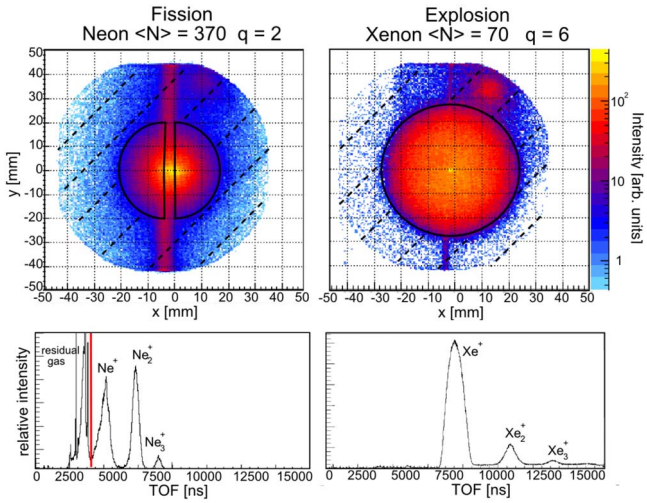

FIG. 1. (Color online) Detector images (top) and TOF spectra (bottom) for neon cluster fission (left) and of xenon cluster explosion (right). For the detector images the logarithmic z scale represents the relative intensity in each pixel. The diameters of the fragmentation pattern and the width of the TOF peaks directly reflect the amount of particle momentum. The lines indicate the detector position filters.

located in the interior of the spectrometer, and the charged cluster fragments are guided on time- and position-sensitive detectors by an axial electric extraction field with a $\Omega=4\pi$ detection efficiency. For each detected fragment the mass-to-charge ratio can be measured by the time of flight (TOF). With the time and position data, the full kinematic information of the charged particles is recorded and their momentum vectors can be determined [22,23]. Thus, conclusions about the initial fragmentation dynamics can be drawn. For further analysis only those events are used for which the total number of detected ions matches the dominant highest-charge states expected from the photoionization process.

The ion detector images and TOF spectra for the two most opposite cases, Ne fission and Xe explosion, are shown in Fig. 1. Both images clearly show a projected sphere of cluster fragments around the detector center over a low background. For both detector images (top panel in Fig. 1), the passing synchrotron light beam can be identified as a vertical line. For the fission case the background features are more pronounced due to the higher photoionization cross section of the residual gas at $h\nu$=80 eV. The distribution of cluster fragments appear isotropic on the detector, i.e., in the laboratory frame of reference, for both cases. The size of the sphere, however, directly reflecting the particle momentum, is much larger for the explosion than for the fission conditions. The TOF spectra in Fig. 1 show very different fragment intensities for the fission and explosion cases, indicating different fragmentation channels. For discussion of the fragmentation channels, detector position filters are applied to the data as indicated in Fig. 1 in order to eliminate the signal from the residual gas. In the four panels of Fig. 2 the coincident cluster fragments are plotted against each other for the fission and explosion regime for both Ne and Xe. In the cases where only two initial charges are generated, the first detected fragment (first type) is plotted versus the sec-

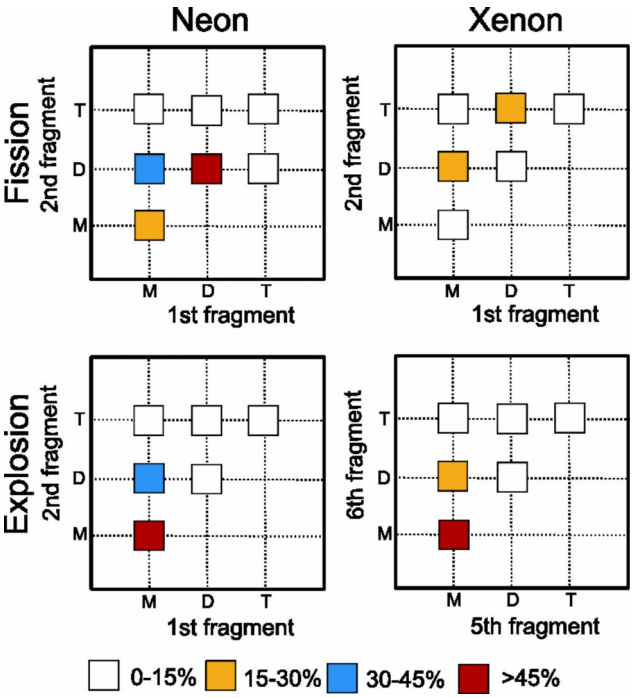

FIG. 2. (Color online) Ne and Xe decay channels for fission and explosion as explained in the text. The x and y axes show the type, i.e., M, monomer, D, dimer, and T, trimer of the first and second fragments, respectively. For Xe explosion the first four fragments are predominantly monomers and therefore the fifth vs the sixth fragments is shown. The shading represents the relative occurrence of the fragments.

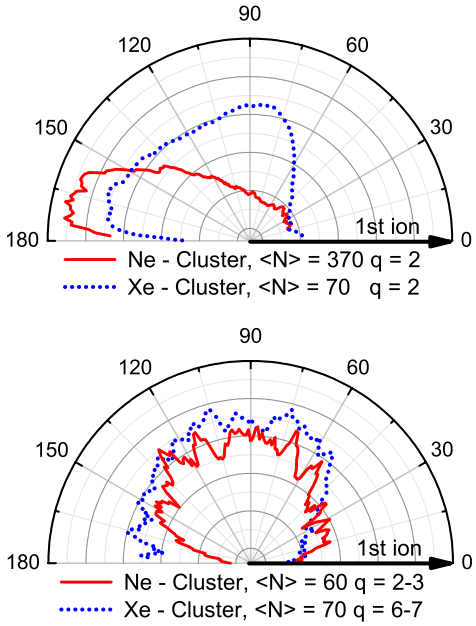

FIG. 3. (Color online) Dissociation angles of Ne (solid line) and Xe (dotted line) clusters for the fission (top) and explosion (bottom) regimes. The direction of the first detected fragment is symbolized by an arrow. The angles of the following fragments are plotted relative to this direction.

ond fragment (second type). For Xe explosion, where there are six charges generated on the cluster, the graph has to be reduced in its dimensions. Data analysis shows, that the first four fragments of the Xe explosion are more than 75% monomers. Therefore only the decay channels of the fifth versus the sixth fragment are shown. Figure 2 shows that for fission preferably dimers or trimers are produced and that no larger fragments can be observed. This is in good agreement with previous experimental investigations on rare gas clusters [8,24] but differs from the predictions of the classical fission process into a few large fragments [1]. For explosion, the signal is predominantly due to monomers. Very generally speaking, however, the observed trend from larger fragments in the case of fission to many small fragments in case of explosion agrees with the theoretical predictions [1,3,4].

With the kinematic information of all charged particles the analysis of the fragmentation geometry in the cluster frame of reference becomes possible. To do so, the momentum vector of the first detected fragment is used to define a reference axis for all the following ones and the angles between the fragments are calculated from their scalar product. The fragment angle distribution data is normalized with $(\sin\theta)^{-1}$ for the solid angle element. The resulting angle distributions averaged over all decay channels are plotted in Fig. 3. The momentum vector of the first fragment points toward zero degrees and the distribution of relative angles for all subsequent fragments are shown. While in the laboratory frame of reference the fragment distribution appears always isotropic (Fig. 1), in the cluster frame of reference distinct differences between the fission and explosion regimes become apparent (Fig. 3). For the liquid Ne cluster fission ($q=2$, $\langle N\rangle=370$, $X=0.8$), a very anisotropic fragmentation geometry along one axis is apparent, similar to that of macroscopic liquid drops [5]. This geometry is indicative of the fission process [1]. The angular distribution of the solid Xe clusters (dominant decay channel $q=2$, $\langle N\rangle=70$, $X=0.7$), however, is much more isotropic and deviates from the liquid systems. It should be mentioned, that the observed fragmentation geometry does not simply reflect a mixing with the minor decay channel involving the $q=3$ cluster final state. For three charges a preferred fragment angle of 120 would be expected where no maximum can be observed. Further, the size distribution of the clusters may lead to a mixture of decay processes. Typically, the width of the rare gas cluster size distribution equals N. The fissility parameter scales with $1/N$ and thus the impact would be similar for both systems. While a mixture of decay processes due to the size distribution cannot be excluded for the data, it cannot explain the presently observed differences for the Ne and Xe systems. In the explosion regime (Ne, $q=2-3$, $\langle N\rangle=60$, $X>4.8$; Xe, $q=6-7$, $\langle N\rangle=70$, $X>6.6$), both systems disintegrate isotropically, in good agreement with the calculations [1]. In this context it is interesting to recall that for Ne mainly the cluster size has been reduced and that the decay channels lead to a $q=2$ (70%) or $q=3$ (30%) final state. The observed isotropic fragmentation angles do not reflect the simple Coulomb repulsion of two or three charges, indicating very different fragmentation dynamics from the fission regime.

The angular information is complemented with the charge separation distances (CSDs) of the fragments. The CSD is the distance at which the particles start to be freely acceler-

ated in their respective Coulomb fields. It can be deduced from their measured average kinetic energy release [8]. In the calculation equal distances between all charged particles are assumed. The largest CSD with 9.8 Å is measured for the case of Ne fission, and compares to a bond length of only 3.2 Å. These data suggest that the charges migrate from the excited atom to the neighboring atoms. Due to their high mobility in the liquid cluster, the charged atoms can move in opposite directions before the cluster breaks up and the charged fragments are ejected. In contrast, the CSD for Xe fission is rather short and equals the Xe bond length of 4.3 Å. Therefore the ions cannot redistribute within the cluster but are ejected from their original positions and they can scatter with the neighboring atoms. Other processes such as sequential fragmentation of the clusters can be excluded due to the short CSD. This observation is in agreement with the more isotropic fragmentation geometry of the Xe cluster. The fragmentation geometry (Fig. 3) and the CSD analysis indicate that only the liquid Ne system is in good agreement with the theoretical predictions [1,3,4] and that solid van der Waals systems show a strong deviation from the ideal behavior.

While there is a large difference in the fission regime for the liquid Ne and solid Xe clusters, they show a comparable behavior for their explosion ($X>1$). Here, the CSD for Ne is 3.6 Å, (about one bond length), and for Xe 6.8 Å. The slightly larger CSD of about 1.5 atomic distances for the Xe explosion can be understood by the large number of charges being generated on the excited atom, leading to charge transfer to outer atoms or expansion of the cluster before its final breakup. The observed short CSD and similarly the isotropic fragment distribution (Fig. 3) are in good agreement with the calculations [1,3,4]. The data show that in the explosion regime the cluster phase and atom mobility do not alter the fragmentation dynamics.

In conclusion, the fragmentation of liquid Ne and solid Xe clusters around the Rayleigh instability barrier have been investigated with a momentum-resolving reaction microscope. For $X<1$, i.e., in the fission regime, the predicted anisotropic fragmentation along one axis and large charge separation distances are found only for liquid Ne clusters with high atom mobilities. The fission pattern of solid Xe clusters becomes already much more isotropic with increased kinetic energies, indicating that the ionic fragments are ejected from their original atom positions. For $X>1$, i.e., explosion, both systems show an isotropic spatial distribution of small ionic fragments with high kinetic energies, in good agreement with the calculated predictions. The data show that for the fission regime the short-range interaction plays an important role for the spatial distribution of the fragments and their ejection energies.

We would like to thank all Hasylab staff, in particular Hubertus Wabnitz and Ernst Untiedt, for their outstanding support, as well as Tim Laarmann (MBI) for the use of his cluster source and Daniel Rolles (LBNL) for interesting discussions. Funding is acknowledged from BMBF Grant No. 05KS4KTC1 and HGF Virtuelles Institut Grant No. VH-VI-103.

[1] I. Last, Y. Levy, and J. Jortner, Proc. Natl. Acad. Sci. U.S.A. **99**, 9107 (2002).
[2] L. Rayleigh, Philos. Mag. **14**, 184 (1882).
[3] I. Last, Y. Levy, and J. Jortner, J. Chem. Phys. **123**, 154301 (2005).
[4] J. Jortner, L. Isidore, and Y. Levy, Int. J. Mass. Spectrom. **249-250**, 184 (2006).
[5] D. Duft, T. Achtzehn, R. Müller, B. A. Huber, and T. Leisner, Nature (London) **421**, 128 (2003).
[6] E. Giglio, B. Gervais, J. Rangama, B. Manil, B. A. Huber, D. Duft, R. Müller, T. Leisner, and C. Guet, Phys. Rev. E **77**, 036319 (2008).
[7] I. Mähr, F. Zappa, S. Denifl, D. Kubala, O. Echt, T. D. Märk, and P. Scheier, Phys. Rev. Lett. **98**, 023401 (2007).
[8] E. Rühl, Int. J. Mass. Spectrom. **229**, 117 (2003).
[9] T. Ditmire, J. Zweiback, V. P. Yanovsky, T. E. Cowan, G. Hays, and K. B. Wharton, Nature (London) **398**, 489 (1999).
[10] V. G. Baidakov, Sov. J. Low Temp. Phys. **10**, 353 (1984).
[11] J. A. Barker, Mol. Phys. **80**, 815 (1993).
[12] K. Sattler, J. Mühlbach, O. Echt, P. Pfau, and E. Recknagel, Phys. Rev. Lett. **47**, 160 (1981).
[13] O. F. Hagena and W. Obert, J. Chem. Phys. **56**, 1793 (1972).
[14] J. Wörmer, V. Guzielski, J. Stapelfeldt, and T. Möller, Chem. Phys. Lett. **159**, 321 (1989).
[15] H. Haberland, Surf. Sci. **156**, 305 (1985).
[16] F. Federmann, O. Björneholm, A. Beutler, and T. Möller, Phys. Rev. Lett. **73**, 1549 (1994).
[17] T. Jahnke *et al.*, Phys. Rev. Lett. **93**, 163401 (2004).
[18] L. O. Werme, T. Bergmark, and K. Siegbahn, Phys. Scr. **6**, 141 (1972).
[19] H. Körber and W. Mehlhorn, Phys. Lett. **13**, 129 (1964).
[20] R. von Pietrowski, M. Rutzen, K. von Haeften, S. Kakar, and T. Möller, Z. Phys. D: At., Mol. Clusters **40**, 20 (1997).
[21] C. U. S. Larsson, A. Beutler, O. Björneholm, F. Federmann, U. Hahn, A. Rieck, S. Verbin, and T. Möller, Nucl. Instrum. Methods Phys. Res. A **337**, 603 (1994).
[22] R. Dörner, V. Mergel, O. Jagutzki, L. Spielberger, J. Ullrich, R. Moshammer, and H. Schmidt-Böcking, Phys. Rep. **330**, 96 (2000).
[23] J. Ullrich, R. Moshammer, A. Dorn, R. Dörner, H. Schmidt, and H. Schmidt-Böcking, Rep. Prog. Phys. **66**, 1463 (2003).
[24] H. Murakami, K. Nagaya, Y. Ohmasa, H. Iwayama, and M. Yao, J. Chem. Phys. **126**, 054306 (2007).